DAMAGE DETECTION OF THE 2008 SICHUAN, CHINA EARTHQUAKE FROM ALOS OPTICAL IMAGES

Wen Liu, Fumio Yamazaki
Department of Urban Environment Systems, Graduate School of Engineering,
Chiba University, 1-33, Yayoi-cho, Inage-ku, Chiba, Chiba, 263-8522 Japan
Liu <nanahachimizu@yahoo.co.jp**>, Yamazaki <**yamazaki@tu.chiba-u.ac.jp**>**

KEY WORDS: The 2008 Sichuan Earthquake, Damage detection, ALOS, AVNIR-2, Landslide

ABSTRACT: Damage detection is carried out from ALOS optical images that captured the stricken areas by the Sichuan, China earthquake, which occurred on May 12, 2008. Since landslides occurred extensively in this earthquake, we try to extract the landslide areas comparing the pre- and post- event images of ALOS/AVNIR-2. First, a level-slice method is used to extract vegetated areas and water areas. Then, the bare ground areas are detected from the pre- and post- event images by a pixel-based classification, after masking vegetation and water. Then the difference of the bare ground between two images is considered as landslides. The rise of water-level in the river is also detected in the areas where landslides dammed off the river flow. The digital elevation model from SRTM is also employed in this study to investigate the relationship between the slope angle and the occurrence of landslide.

1. INTRODUCTION

The Sichuan, China earthquake with magnitude 7.9 occurred on May 12, 2008 （USGS）. Due to this earthquake, approximately ninety thousand people were killed or missing and 374,000 people were injured. Since the epicenter is located in a mountainous area, the roads and rivers were blocked by landslides. Many villages in the mountains were isolated, and landslide lakes threatened the people's lives. It is very important to grasp the extent of damage at an early stage and take a quick response soon after a disaster. The affected areas were large and the approach from roadways was difficult. Thus, remote sensing technology is an effective way to grasp damage distribution in this event.

The visual interpretation of high resolution satellite images, e.g. IKONOS, QuickBird, has been used extensively to extract actual landslides visually and produce landslide-risk maps. This method can obtain highly accurate results, but very time consuming. Hence a change detection technique (Lu et al., 2004) is applied as an effective automated method for detecting landslides. Miura et al. (2008) evaluated landslides by comparing the difference of the normalized difference vegetation index (NDVI) before and after an earthquake from IKONOS images. Jaya et al. (2005) applied a multi-temporal Principal Component Analysis to detect the decrease of vegetation cover by landslide from SPOT/HRV images. The shortcoming of this method is the necessity of the images covering the same area before and after a disaster. Danneels et al. (2007) used supervised classification methods to detect landslide from one ASTER scene (3 VNIR and 6 SWIR bands). Other than these papers, there are a number of researches on landslide detection.

In this study, the detection of landslides and river water-level changes is carried out by a band threshold and a pixel-based classification from ALOS/AVNIR-2 images, obtained before and after the 2008 Sichuan, China earthquake.

2. DATA USED AND FLOW OF THE STUDY

The Advanced Land Observing Satellite (ALOS) is Japanese Earth observation satellite, which

was launched in January 2006 by Japan Aerospace Exploration Agency (JAXA). ALOS has three sensors: the Panchromatic Remote-sensing Instrument for Stereo Mapping (PRISM) for digital elevation mapping, the Advanced Visible and Near Infrared Radiometer type 2 (AVNIR-2) for precise land coverage observation, and the Phased Array type L-band Synthetic Aperture Radar (PALSAR) for day-and-night and all-weather land observation (JAXA homepage).

AVNIR-2 images used in this study are the pre- and post- event images covering the northern Beichuan county, Sichuan province, China, as shown in Figure 1. AVNIR-2 has three visible (BGR) and one near infrared (NIR) bands, with 10m spatial resolution. The pre-event image was taken on March 31, 2006 and the post-event one on May 26, 2008. The size of images used was 2000×1000 pixels, covering about 200 km^2. A digital elevation model (DEM) from Shuttle Radar Topography Mission (SRTM) by NASA is also employed to investigate the occurrence condition of landslides. The data is referred to as SRTM-3, which is sometimes called "90m data" since 3 arc-second at the equator corresponds to roughly 90m in horizontal extent.

The flow of this study is shown in Figure 2. First, the pre- and post- event images are co-registered. Then, the NDVI values are calculated from the two images. Employing the thresholds for the NDVI and the NIR band's digital number, water and vegetation areas are extracted. Comparing the extracted water areas from the pre- and post-event images, the difference of water-level and flooded areas are detected. Then, supervised classification by the

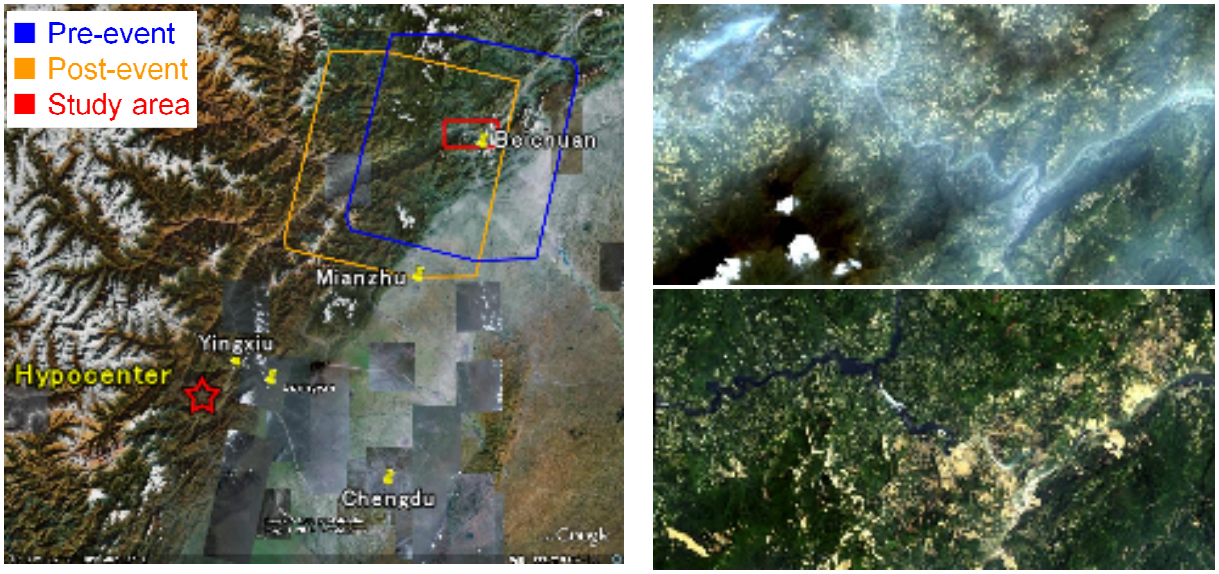

Figure 1 ALOS/AVNIR-2 images before (top) and after (bottom) the 2008 Sichuan earthquake

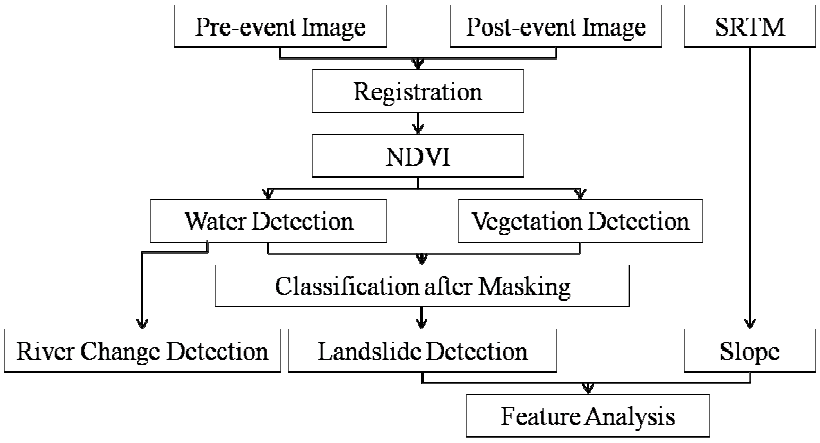

Figure 2 Flow of this study

maximum likelihood method is carried for the remaining part of the images. After masking the water areas and the vegetation areas, extracted by high NDVI values, bare ground areas are extracted. The increased bare ground areas after the earthquake are considered as landslides. Finally, SRTM-3 data is used to investigate the relationship between the occurrence of landslides and the slope angle.

3. CHANGE DETECTION

3.1 Registration

To detect the difference of the result of the pixel-based classification for the pre-event and post-event images, registration is an important first step. Since the change of elevation is very large in this area, orthorectification is desirable. But high-resolution DEM data is not available. Hence, orthorectification was not carried in this study. Using 12 ground control points along the bottom of the valley, two images were coregistered as much as possible. In this method, the peaks of the mountain cannot be coregistered, and thus the maximum registration error is about 1.5 pixels in these areas.

3.2 River Changes Detection

Since water shows lower NDVI values than others, a NDVI threshold was introduced to extract water areas. First, the NDVI values for the pre- and post-event images were calculated. The two images were taken in different seasons (March 31 for pre-event and May 26 for post-event), the NDVI values show a big difference: in the range -0.46 – -0.17 for pre-event and that -0.53 – +0.59 for post-event.

In the pre-event NDVI image, shadow and water show low NDVI values. The areas in the shadow of mountains show lower NDVI values than the surrounding areas. The pixels with NDVI value lower than -0.35 are considered as water. Since the areas covered by the shadow of cloud also show low NDVI values, noise removal is needed. By an object-based method (Vu et al., 2006), river-water can be extracted as a long and big object. The noise generated by misregistration can be removed by its size. Since the maximum registration error is about 1.5 pixels, the objects smaller than 2×2 pixels were removed as noise.

In the post-event NDVI image, water and landslide show the lowest NDVI value. Since landslide often occurred near the river, it is difficult to discriminate landslide and water by the NDVI value. Thus, the near-infrared (NIR) band was employed to extract water in the post-event image because water shows the lowest value in the NIR band than in the other bands. The pixels with NIR's digital number (DN) lower than 35 were extracted as water. The noise due to misregistration was also removed by the object-based method.

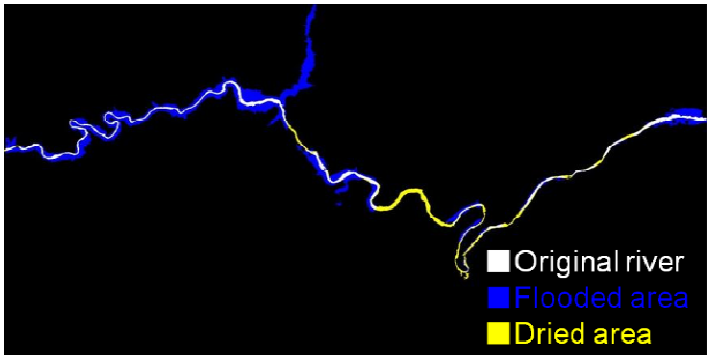

Figure 3 Water-level changes in the river after the earthquake

Comparing the extracted water areas from the pre- and post-event images, the change of the river can be detected. Figure 3 shows a color composite image assigning red and green to the pre-event water area and blue to the post-event water area. In the figure, blue areas represent those flooded after the earthquake due to landslide dams, yellow (red+green) areas those dried after the earthquake, e.g. filled by landslide, and white areas those unchanged. The river-water is 2.07 km^2 in the pre-event image while that is 5.45 km^2 in the post-event one. The breakdown of the change is the flooded area (4.08 km^2) and the dried area (0.71 km^2). Due to the landslide dam, the water-level of the river rose and the river-water area became more than twice. Some villages were flooded by water.

3.3 Landslide Detection

To detect landslide, a pixel-based classification was carried for the pre- and post-event images. Masking of water and vegetation was carried out before the classification to raise the accuracy. Since vegetation shows the highest NDVI value in the images, the areas with high NDVI values were assumed as vegetation: larger than -0.25 in the pre-event image and larger than -0.05 in the post-event image.

The extracted water and vegetation areas were masked from the pre- and post-event images. Then the maximum likelihood classification was carried for the remaining part of the images. In the pre-event image, five classes were assigned: vegetation, village, cloud, dry riverbed, bare ground. Since some vegetation areas were in the shadow of mountains and exhibit low NDVI values, they could not be extracted in the step of NDVI threshold. In the post-event image, four classes were assigned: vegetation, village, bare ground, and dried river (soil on river). The results of the classification are shown in Figure 4.

In the result for the pre-event image, the classes of village and dry riverbed could not be distinguished clearly due to mixed-pixel. Since the spatial resolution of AVNIR-2 is 10m and buildings in the village are mostly smaller than $10 \times 10 m^2$, one pixel in the image includes both

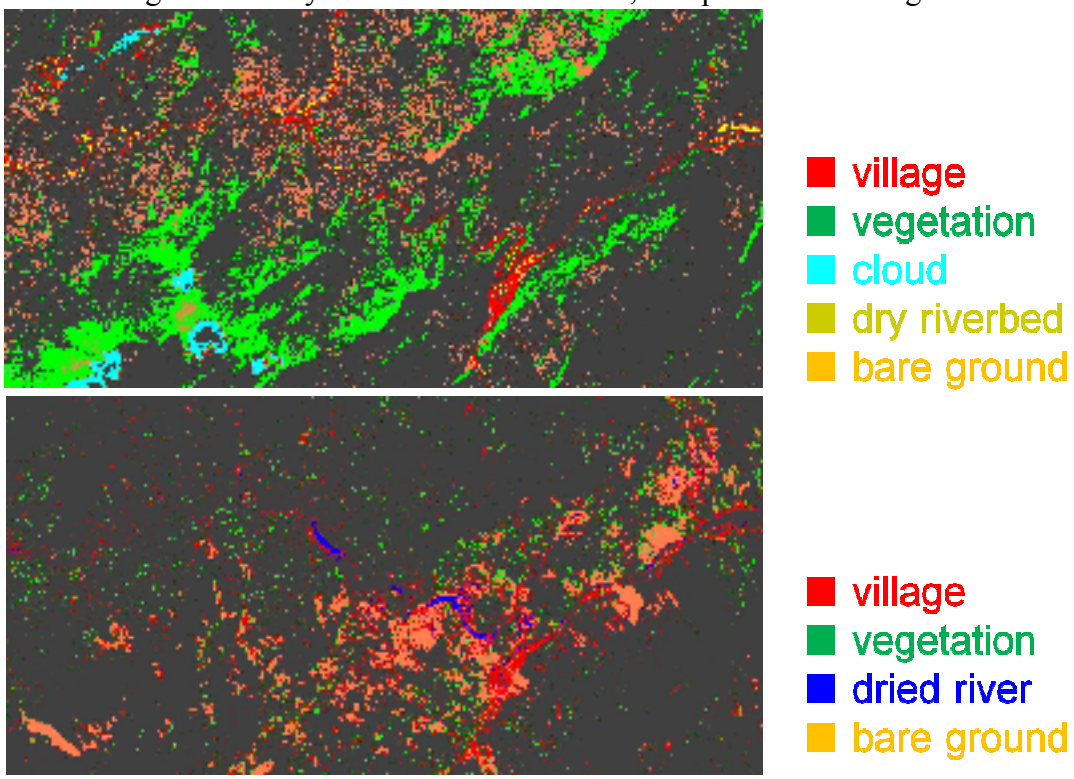

Figure 4 Results of classification for the pre- (top) and post-event (bottom) images

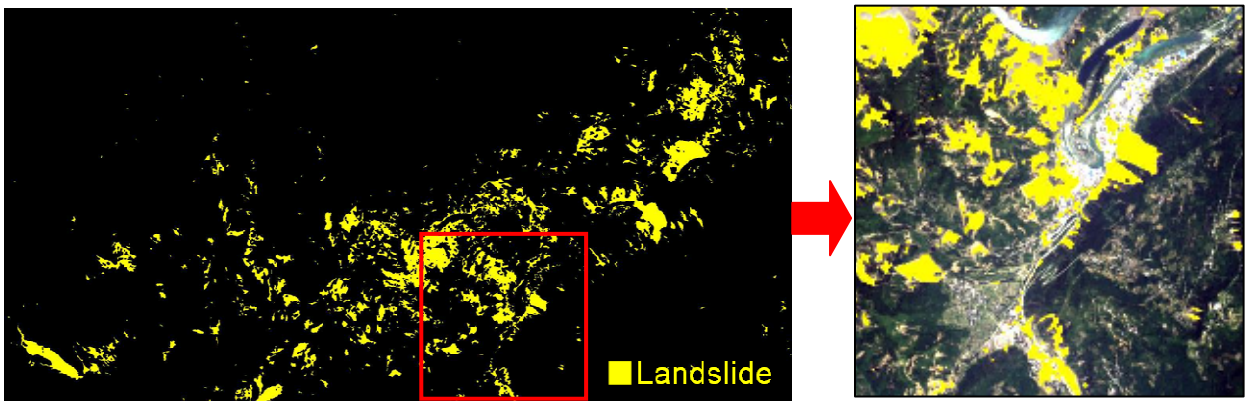

Figure 5 Result of landslide detection and comparison with the post-event image

buildings and surrounding ground. Thus, the village area shows the similar reflectance as ground, and hence it is difficult to discriminate them.

Comparing the extracted bare ground pixels in the pre- and post-event images, the increased pixels after the earthquake were considered as landslide. After removing misregistration noise by the object-based method, the extracted landslide areas shown in Figure 5 are about 11 km^2. Overlapping the result on the post-event image, the shapes of detected landslides look reasonable. Almost all the landslides were detected, but some small ones, smaller than 2×2 pixels, could not be detected due to the noise removal. A village hit by a landslide (Qushan zhen) could also be detected. From the class of dried river in the post-event image, a landslide dam could be detected.

3.4 Relationship between Landslide and Topography

The occurrence of landslide is investigated comparing with topography. The pre-event SRTM data was used as the digital elevation model (DEM) in which the height in the image varies from about 600m to 2,400m. The change of elevation is quite large in this mountainous area. Overlapping the satellite images on the DEM, the 3D image can be obtained as shown in Figure 6. It is observed that landslides mostly occurred on steep slopes.

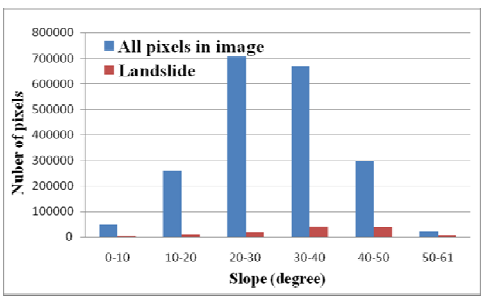

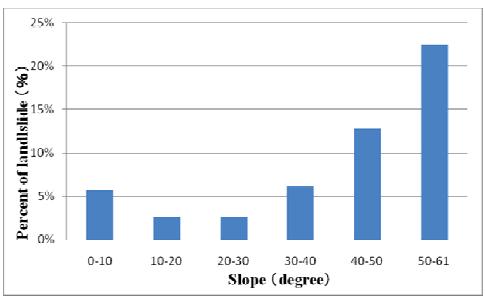

Figure 6 Plot of landslide on 3D model (top) and the relationship between the slope angle and landslide occurrence (bottom)

The slope angle was calculated from the DEM data. There are many high mountains in this area and the slope angle distributes from 0 to 60 degrees; the angle from 20 to 40 degrees shares the most part. The relationship between the slope angle and landslide occurrence is also shown in Figure 6. It is seen that the percentage of landslide areas becomes larger as the slope angle gets steeper.

4. CONCLUSIONS

The detection of landslide and river-water changes was conducted using ALOS/AVNIR-2 images obtained before and after the 12 May 2008 Sichuan, China earthquake. In river change detection, water areas were detected easily by the threshold of NDVI values. But for the landslide which occurred near the river, the near-infrared band worked better than the NDVI threshold. In the landslide detection, land cover classification was carried out after masking water and vegetation areas. Most landslides were extracted reasonably by taking the difference of the extracted bare ground pixels from the pre- and post- event images. Using SRTM data, the occurrence of landslide was found to be related to the slope angle.

Since the objects smaller than 2×2 pixels were removed as noise in this study to eliminate the effect of misregistration, the landslide smaller than $400m^2$ cannot be detected. The limitation of spatial resolution also affected the result of classification. In a further research, the accuracy of the classification should be examined using high-resolution satellite images. Orthorectification using a finer DEM data will reduce the error due to misregistration.

ACKNOWLEDGMENTS

The authors express their gratitude to Japan Aerospace Exploration Agency (JAXA) for providing the ALOS satellite images used in this study.

REFERENCES

Danneels, G., Pirard, E., Havenith, H.B., 2007. Automatic landslide detection from remote sensing images using supervised classification methods. Geoscience and Remote Sensing Symposium. IGARSS 2007. IEEE, pp. 3014-3017.

JAXA, URL: http://www.eorc.jaxa.jp/ALOS/about/avnir2.htm

Jaya, I., and Abe, N., 2006. Methods for Detecting Landslide within Mountains Area Using Multitemporal SPOT HRV Imageries: A Case Study in Niigata, Japan. Study Report of Faculty of Agriculture, Niigata University, Vol. 58, No. 2, pp.109-116.

Lu, D., Mausel, P., Brondizio, E., and Moran, E.F., 2004. Change Detection Techniques. International Journal of Remote Sensing, Vol. 25, No. 12, pp. 2365-2407.

Miura, H. and Midorikawa, S., 2008. Detection of Slope Failure Areas Using High-Resolution Satellite Images and Digital Elevation Model for the 2004 Niigata-Ken Chuetsu, Japan Earthquake. Proceedings of 5th International Conference on Urban Earthquake Engineering, pp.559-564 .

USGS, URL: http://earthquake.usgs.gov/eqcenter/recenteqsww/Quakes/us2008ryan.php

Vu, T.T., Yamazaki, F., and Matsuoka, M., 2006. Object-based extraction of building features from LiDAR and aerial photograph - MORPHSCALE method. 4th International Workshop on Remote Sensing for Post-Disaster Response, Cambridge, UK.
http://www.arct.cam.ac.uk/curbe/4thInt_workshop.html